Petroleum and Coal

Article Open Access

Petrophysical and Geological Modelling of a Marginal Field in the Onshore Debobelt, Niger Delta

I. J Ofoh[1]., R. U Ideozu[2], S. O Onyekuru[1], C. Z Akaolisa[1], A. I Opara[1], C. C Agoha[1], and A. E Okoli[1]

[1] *Department of Geology, Federal University of Technology, P.M.B 1526, Owerri, Imo State, Nigeria*
[2] *Department of Geology, University of Port Harcourt, P.M.B 5323, Choba, Rivers State, Nigeria*

Received May 16, 2023; Accepted July 20, 2023

Abstract

In order to reevaluate the reservoirs identified in an onshore marginal field in the Niger Delta Basin and determine the reserves that are now available, the research combined information from seismic interpretation and petrophysics of four wells. Interpretation of gamma ray curves revealed blocky log motifs typical of sedimentary sequences deposited in a fluvial to shoreline environment. Stratigraphic interpretations showed laterally extensive reservoir intervals, characteristic of foreshore to lower shoreface setting. The objective reservoir intervals' estimated petrophysical variables were porosities (Ø) ranging from 25.9 to 33.1%, shale volume (V_{sh}) ranges between 0.204 and 0.430, and water saturation (Sw) values between 0.204 and 0.430. Reservoir sands "A", "B", "C" and "E" displayed superb porosity, while moderate porosity values were observed in sand "D", "F", "G", "H" and "1" reservoirs. According to the projected hydrocarbon in-place volume, there is a lot of room for further drilling expeditions in this field.

Keywords: *Niger Delta; Seismic; Reservoir sand; Net pay.*

1. Introduction

The research on the characteristics of rocks and how they relate with gases, liquids, and hydrocarbons with reservoir porosity and permeability is known as reservoir petrophysics. It is regarded as the main important physical attribute in terms of fluid storage and transmission [1]. The presence of pores is an indicator of area in a rock that is not filled by the solid matrix. Sandstone reservoirs' porosity may be impacted by an array of factors, like the particle's shape, sorting, and how the grains are packed [2]. Other contributing factors that affect reservoir porosity may include increased cementation and other post-depositional processes [3]. [Grain dimensions have a significant impact influencing the ability of a porous medium to allow easy flow of fluids without changing the structure or displacing any part of the medium. This quantity is known as the permeability of the medium [2-3]. In consequence of this, tiny particles have narrower pore throats than broader grains, consequently finer sandstones have lower permeability than coarser sandstones. Hence, the intent of the research is to conduct a field re-evaluation of the hydrocarbon-bearing sands utilizing a combined petrophysical and seismic technique.

2. Research location

The research location lies in the Northern Depobelt, which consists of the portion of the Niger Delta Basin that lies on land. (Figure 1).

2.1. Regional geology of the Niger Delta

The Akata, Agbada, and Benin Formations constitute the three fundamental formations that make up the stratigraphy of the Niger Delta Basin. [4]. The petroleum source rock was investigated in the Niger Delta Basin, and reported that they contain mixed/humic type kerogen [5]. The reservoir for the generated hydrocarbons comprises mostly of sandstone facies of the Agbada Formation, while the growth faults and rollover anticlines provide the traps preventing the hydrocarbons from escaping to the surface. Sediments were deposited in a series of depo-axes or depobelts [6], controlled by rate of subsidence and gravity tectonics [7]. Detailed studies on the seismic and well log interpretation in the Niger Delta Basin, have been documented by [8-10].

3. Dataset and method of interpretation

3.1. Dataset

The dataset used in this study include wireline log of 4 wells, a deviation survey, check-shot, base map and a 3D seismic (seg-y) of four hundred and sixty-one inlines and four hundred and forty-one crosslines. Software from Petrel and Landmark Geographics, respectively, was used for the study of the geophysical data and seismic interpretation.

3.2. Approach to interpretation

3.2.1. Base map of the research location

The base map displays the wells position and orientation see (Figure 1).

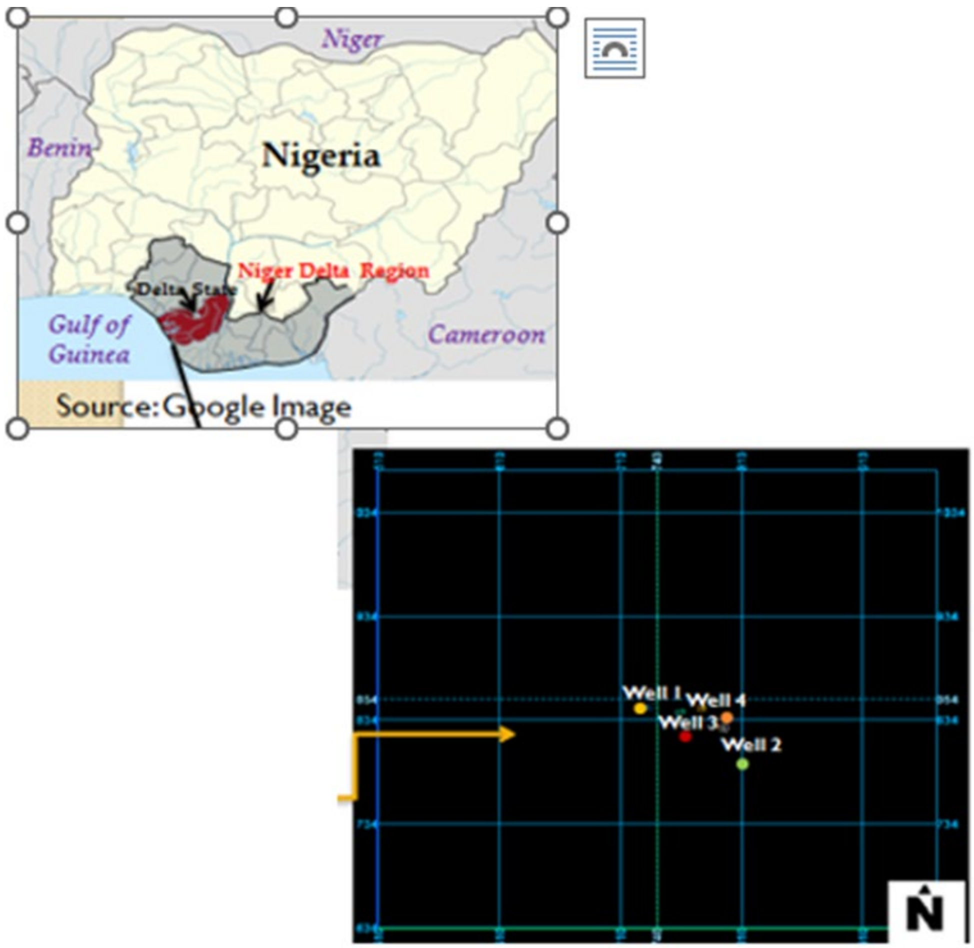

Fig. 1. Map of the analyzed field's seismic activity showing the precise locations of the investigated wells.

3.2.2. Approach to formation evaluation

Lithology correlation of the 4 wells was achieved using the combination of gamma ray and resistivity logs, while fluid types in each of the mapped reservoir intervals was determined using the resistivity curves. Porosity, H_2O saturation, V_{sh}, net-pay thickness, and net/gross ratio are some of the petrophysical characteristics that were determined.

The mathematical models employed to analyze the formation and estimate the reservoir's attributes include:

(i) Porosity measures how much empty space there is relative to the whole volume of the rock [11].

porosity(Ø)= Volume of pores/Total volume of rock (1)

(ii) The Archie's model for H_2O saturation [12]

$S_w = (F \times R_w/R_t)^{1/n}$. (2)

where S_w is H_2O saturation, F is the formation volume factor, R_w is the formation H_2O resistivity, R_t is the true resistivity of the formation, while n is the saturation (usually taken to be 2.0).

(iii) Shale volume (V_{sh}) in the reservoirs was calculated from the lithology log by the gamma ray index using the equation below;

$I_{GR} = {}^{GRlog - GR\,min}/_{GRmax - GRmin}$ (3)

where: GR_{max} = highest recorded GR reading and GR_{min} = lowest GR reading; I_{GR}= GR index; GR_{LOG} = GR number derived from log.

(iv) Net-pay thickness: Porosity values exceeding ten percent and shale volumes below fifty percent were used to establish the reservoirs. Determination of the net-pay thickness was achieved by the removing the volume of shale (V_{sh}) from the gross reservoir volume.

(v) Net/Gross ratio: In this study, the reservoir's tops and bottoms were used for calculating the gross sand thickness. The non-reservoir sands were mapped out applying the lithology log (gamma ray), which served as the basis for calculating the net to gross ratio. A shale line was used as a cut-off the non-reservoir zone on the gamma ray log.

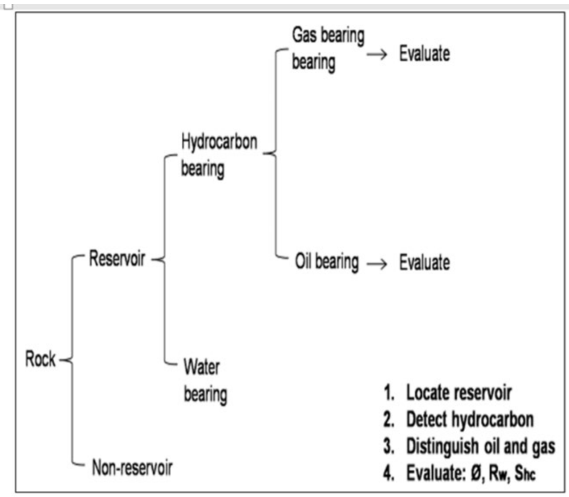

Fig. 2. Flow chart used for log interpretation in the research.

Computable log review was achieved as displayed in (Figure 2) in conjunction to results from the seismic analysis. Empirical relations were harnessed to make geological inferences in the studied reservoir intervals.

3.2.3. Geological model

It was crucial to adjust the seismic section to depth while creating a geologic model, particularly when there were major fluctuations in velocity owing to a lithologic change etc. To a depth transformation to be uncomplicated in this part, velocity is basically led by depth.

3.2.4 Tracing the horizon and seismic analysis

Tracing the horizon and seismic analysis was easy; it began with mapping of "9" horizons ("A-I"). Sand ("A-I") reservoir top was mapped on the well tie-in panel was used as the basis for seismic horizon analysis. The horizons were mapped both in the inlines and crosslines to understand the reservoir structural geometry and compartmentalization. The generated time structure maps from the interpreted horizons were converted to depth maps using appropriate velocity models. The contoured time and depth maps combined with the faults to reveal the structural framework of the field. The depth maps coincided with the reservoir tops from well log correlation, and gave insights on the reservoir structure. The maps were also handy in revealing parts of the reservoir with unswept hydrocarbons for infill drilling. The depth map formed the basis for geological model building in this study.

3.2.5. Estimating oil reserves

Original oil in-place (OOIP) [13]:

$$OOIP = 7758 \times Vol \times (\emptyset) \times (1 - S_w) \quad (4)$$

where: 7758 = change factor from acre-ft to barrel employing the equation; Vol= (h x A);
Vol = net volume; h = pay-thickness from petrophysics; A = area from 3D seismic analysis.

4. Outcome of the findings

4.1. Findings from the lithological correlation

The lithology were essentially sand-shale sequences with simply a couple of transitional names including silts, heteroliths, etc. in some parts. Sands have been separated from log deflections, and lithology log was used to display the presence of shales, which were detected by log diversion to the right to lower values beyond the shale baseline. Correlation of the identified lithologies is presented in Figure 3 and 4.

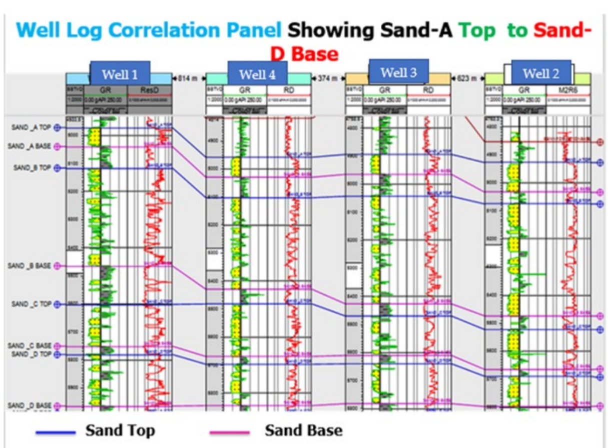

Fig. 3. The well correlation panel of the Marginal Field (Sand-A top-Sand-D base).

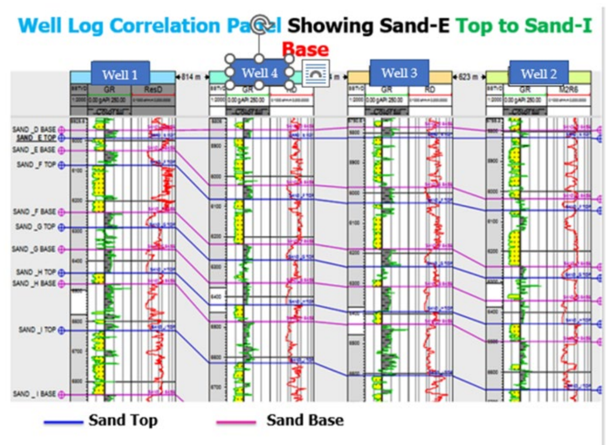

Fig. 4. The well correlation panel for the Marginal Field (Sand-D base-Sand-I base).

4.2. Estimated petrophysical properties

The summary of the estimated petrophysical properties for each of the nine (9) hydrocarbon reservoirs mapped in this study are presented in Tables 1 to 9. The sand reservoirs were designated as Sand-A to Sand-I as presented in Figures 3 and 4. It was observed that the estimated average porosity values for the reservoirs decrease with increasing depth. This could be attributed to increased grain-to-grain contact and the resulting decrease sediment pore spaces due to increased weight of the overburden.

Table 1. Sand-A petrophysical parameters summary.

Parameter	Well-1	Well-3	Well-4	Well-2
Top (ft)	4969.50	4954.50	4894.50	4931.75
Base (ft)	5040.00	5027.75	4962.00	5037.00
Gross sand thickness (ft)	70.500	73.250	67.500	105.250
$V_{sh.}$	0.024	0.017	0.032	0.015
Net-pay (ft)	70.476	73.233	67.468	105.235
Net to gross ratio	0.999	0.999	0.999	0.999
Porosity $_{\emptyset\emptyset}$ (%)	30	30.7	33.1	30.1
S_w	0.228	0.363	0.346	0.392

Table 2. Summary of petrophysical parameters in Sand-B.

Parameter	Well-1	Well-3	Well-4	Well-2
Top (ft)	5116.00	5101.50	5038.00	5072.00
Base (ft)	5463.50	5430.35	5422.50	5474.50
Gross sand thickness (ft)	347.500	328.850	384.500	402.500
$V_{sh.}$	0.086	0.084	0.099	0.050
Net-pay (ft)	347.414	328.766	384.401	402.450
Net to gross ratio	0.999	0.999	0.999	0.999
Porosity $_{ØØ}$ (%)	29.2	31.4	31.9	31.9
S_w	0.299	0.392	0.319	0.400

Table 3. Summary of petrophysical parameters in Sand-C.

Parameter	Well-1	Well-3	Well-4	Well-2
Top (ft)	5613.75	5484.25	5470.00	5520.00
Base (ft)	5750.75	5670.00	5605.50	5664.50
Gross sand thickness (ft)	137.000	185.750	135.500	144.500
$V_{sh.}$	0.071	0.051	0.071	0.055
Net-pay (ft)	136.929	185.699	135.429	144.445
Net to gross ratio	0.999	0.999	0.999	0.999
Porosity $_{ØØ}$ (%)	28.1	29.9	31.7	31.2
S_w	0.305	0.389	0.405	0.406

Table 4. Summary of petrophysical parameters in Sand-D.

Parameter	Well-1	Well-3	Well-4	Well-2
Top (ft)	5778.00	5695.50	5634.50	5689.50
Base (ft)	5964.75	5695.50	5786.00	5805.50
Gross sand thickness (ft)	186.750	151.250	151.500	116.000
$V_{sh.}$	0.084	0.089	0.090	0.066
Net-pay (ft)	186.666	151.161	151.410	115.934
Net to gross ratio	0.999	0.999	0.999	0.999
Porosity $_{ØØ}$ (%)	28.0	29.4	29.5	31.1
S_w	0.274	0.394	0.405	0.372

Table 5. Summary of Petrophysical parameters in Sand-E.

Parameter	Well-1	Well-3	Well-4	Well-2
Top (ft)	5991.50	5873.00	5810.50	5821.50
Base (ft)	6035.75	6027.75	5980.00	6042.50
Gross sand thickness (ft)	44.250	154.750	169.500	211.000
$V_{sh.}$	0.074	0.084	0.058	0.378
Net-pay (ft)	44.176	154.666	169.442	220.622
Net to gross ratio	0.998	0.998	0.999	0.998
Porosity $_{ØØ}$ (%)	28.7	31.4	30.5	31.9
S_w	0.230	0.378	0.306	0.378

Table 6. Summary of Petrophysical parameters in Sand-F.

Parameter	Well-1	Well-3	Well-4	Well-2
Top (ft)	6083.50	6075.25	6034.00	6063.25
Base (ft)	6237.50	6226.50	6185.00	6250.00
Gross sand thickness (ft)	154.000	151.250	151.000	186.750
$V_{sh.}$	0.035	0.025	0.058	0.031
Net-pay (ft)	153.965	151.225	150.942	186.719
Net to gross ratio	0.999	0.999	0.999	0.999
Porosity $_{ØØ}$ (%)	25.9	27.6	26.2	28.5
S_w	0.204	0.369	0.334	0.381

Table 7. Summary of Ppetrophysical parameters in Sand-G.

Parameter	Well-1	Well-3	Well-4	Well-2
Top (ft)	6294.00	6275.75	6232.00	6286.25
Base (ft)	6359.25	6349.50	6311.50	6362.75
Gross sand thickness (ft)	65.250	73.750	79.500	76.500
$V_{sh.}$	0.198	0.220	0.193	0.209
Net-pay (ft)	65.052	73.530	79.307	76.291
Net to gross ratio	0.997	0.997	0.998	0.997
Porosity $_{øø}$ (%)	28.2	29.1	27.9	31.0
S_w	0.330	0.430	0.363	0.345

Table 8. Summary of petrophysical parameters in Sand-H.

Parameter	Well-1	Well-3	Well-4	Well-2
Top (ft)	6440.00	6426.00	6391.00	6438.75
Base (ft)	6475.75	6485.00	6449.00	6508.75
Gross sand thickness (ft)	35.750	59.000	58.000	70.000
$V_{sh.}$	0.019	0.055	0.050	0.055
Net-pay (ft)	35.731	58.945	57.950	69.945
Net to gross ratio	0.999	0.999	0.999	0.999
Porosity $_{øø}$ (%)	27.8	30.7	29.0	30.4
S_w	0.300	0.426	0.400	0.366

Table 9. Summary of Petrophysical parameters in Sand-I.

Parameter	Well-1	Well-3	Well-4	Well-2
Top (ft)	6630.00	6616.00	6607.50	6660.75
Base (ft)	6844.25	6827.25	6793.50	6842.50
Gross sand thickness (ft)	214.250	211.250	186.000	181.750
$V_{sh.}$	0.043	0.046	0.052	0.044
Net-pay (ft)	214.207	211.204	185.948	181.706
Net to gross ratio	0.999	0.999	0.999	0.999
Porosity $_{øø}$ (%)	26.7	28.9	27.8	29.5
S_w	0.342	0.424	0.351	0.398

4.3. Estimated hydrocarbon reserves

Table 10 is a summary of the calculated hydrocarbon volumes for each of the reservoirs evaluated in this study. The total reserve estimation values throughout each reservoir top are therefore outlined below, as shown in Table 10.

Table 10. Showing estimated original oil in place across the reservoir tops

Reservoir tops	Estimated reserve
Sand-A	333.3MMB
Sand-B	3131.6MMB
Sand-C	1145.7 MMB
Sand-D	1198.7 MMB
Sand-E	1254.6 MMB
Sand-F	1214.3 MMB
Sand-G	2433.2 MMB
Sand-H	2076.7 MMB
Sand-I	1165.3 MMB
Total Sum of Original Oil In-Place (OOIP)	13,953.4 MMB

4.4. Result of the seismic interpretation

Figure 5 is a display of an interpreted seismic section (inline 741) showing faults and horizons mapped in the study area. The aerial coverage of the 3D seismic data is approximately 155.5 km^2. Figure 5 also show overlay of the studied wells on the seismic data. This was obtained by importing the checkshot information provided in Well-2 to all the wells, to enable calibration with the seismic data. This was used to ensure accurate mapping of the reservoir sand tops and also to ascertain its stratigraphic continuity in both dip and strike directions.

4.5. Structural framework of the field

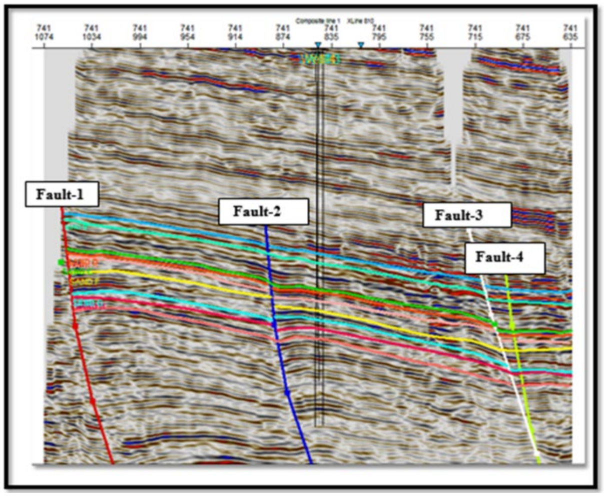

Fig. 5: Using Petrel version 2010, this seismic section of In-line 741 shows the mapped horizons and faults F1, F2, F3, and F4.

The interpreted faults in the study area are presented in Figure 5. The faults gave insights into the structural framework of each of the objective reservoir intervals. In all, four major growth faults were mapped in the field and designated as F1, F2, F3 and F4, respectively. The faults are listric in nature suggesting that they are typical Niger Delta growth structures. The faults were syn-depositional with the sediment deposition in the delta. The faults created accommodation for the deposition of thicker sedimentary packages on the down-thrown side, leading to the formation of roll-over anticlinal structures. Faults F2 and F4 were observed to form fault-dependent traps in the field.

4.6. Time and depth structural maps

The summary Table 11 underneath the image of the time and depth structural map reveals the form of contact as shown in (Figures 6 - 10)

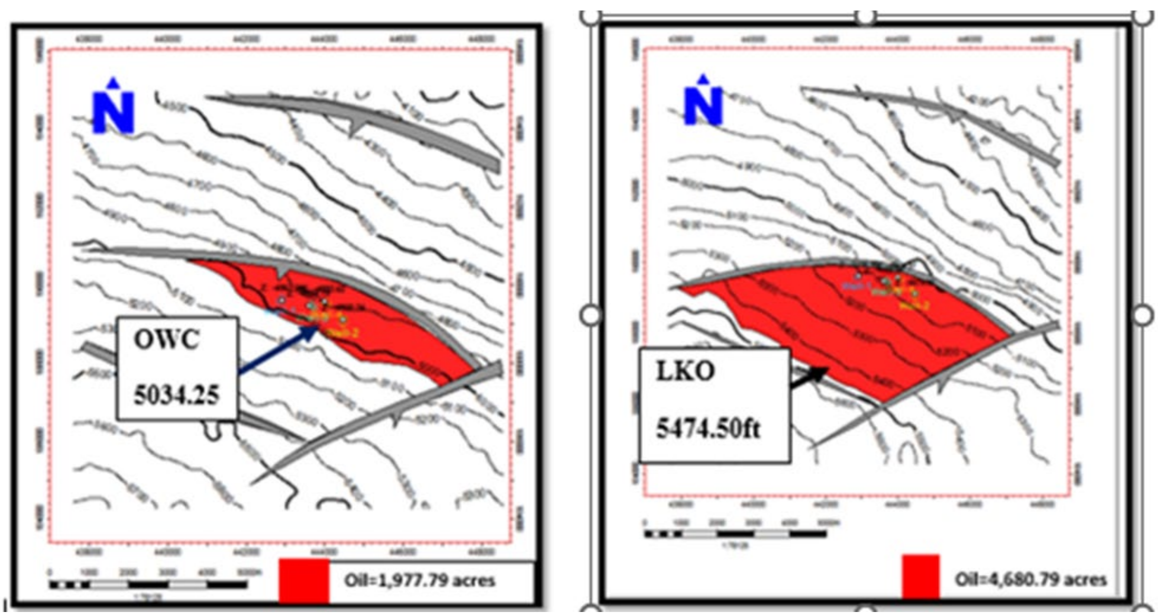

Fig. 6. (a) Oil water contact (OWC) is shown on Sand-A's top-depth structural map, and the lowest known oil (LKO) is shown on Sand-B's top-depth structural map, respectively.

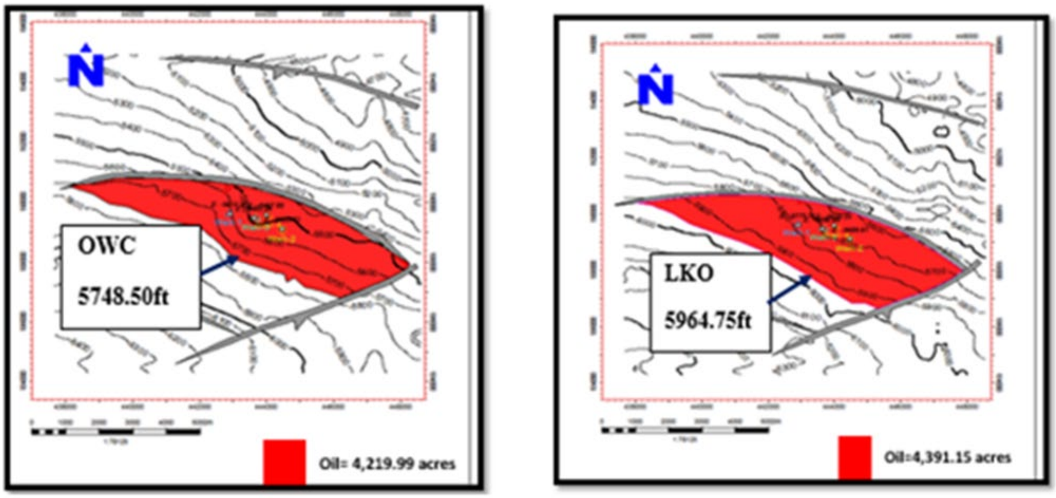

Fig. 7. (a) Oil-water contact (OWC) is shown on the Sand-C top-depth structural map, and the lowest known oil (LKO) is shown on the Sand-D top-depth structural map, respectively.

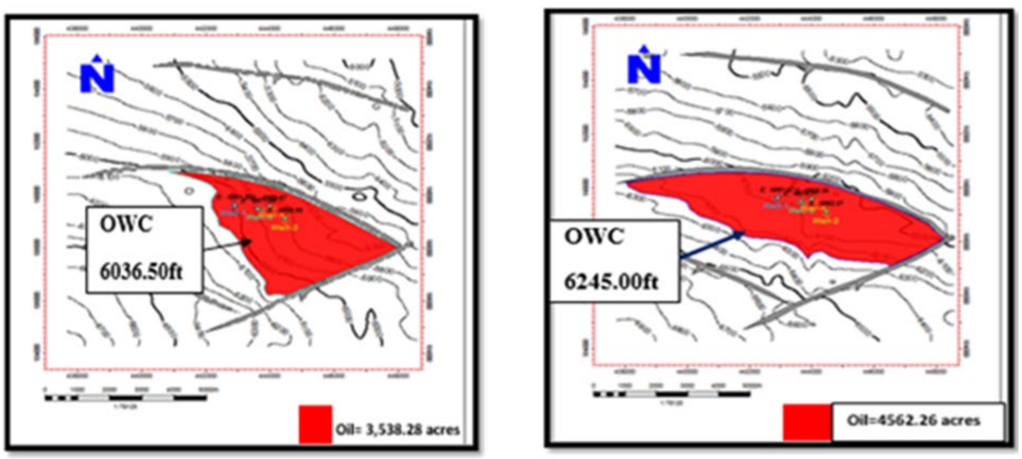

Fig. 8. (a) Oil-water contact (OWC) is shown on the Sand-E top-depth structural map, and it is also shown on the Sand-F top-depth structural map, respectively.

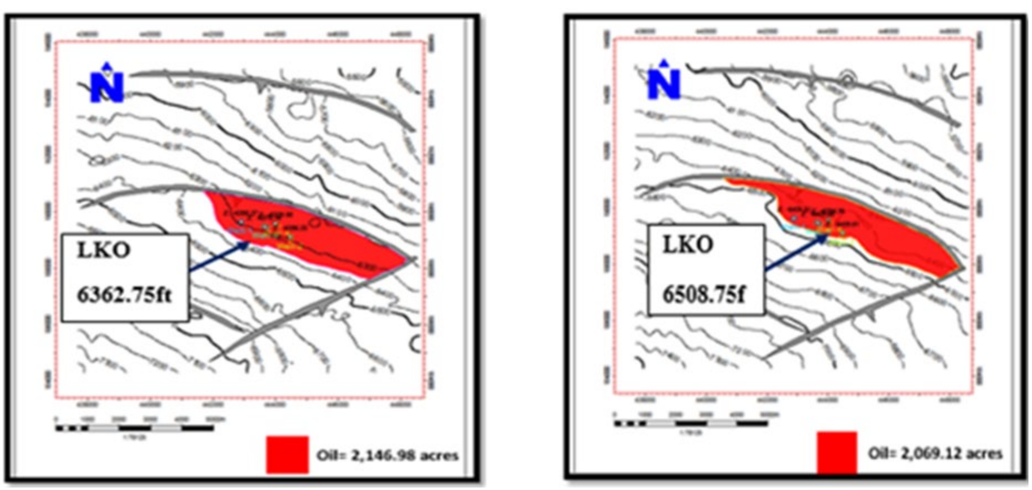

Fig. 9. (a) Both the Sand-G top-depth structural map and the Sand-H top-depth structural map, respectively, reveal the lowest known oil (LKO).

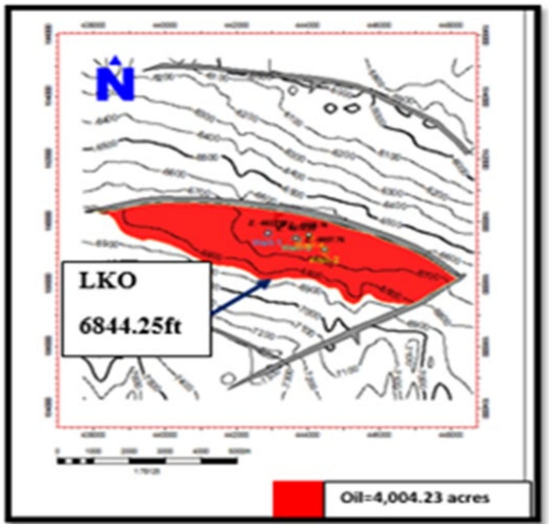

Fig. 10. Lowest Known Oil (LKO) is displayed on the Sand-I top-depth structural map.

Table 11.

Reservior sands	Area extent (acres)	Contact type
Sand-"A"	1,977.80	OWC
Sand-"B"	4,680.80	LKO
Sand-"C"	4,219.99	OWC
Sand-"D"	4,391.15	LKO
Sand-"E"	3,538.28	OWC
Sand-"F"	4,562.28	OWC
Sand-"G"	2,146.99	LKO
Sand-"H"	2,069.13	LKO
Sand –"I"	4, 004.24	LKO

4.7. Reservoir composition

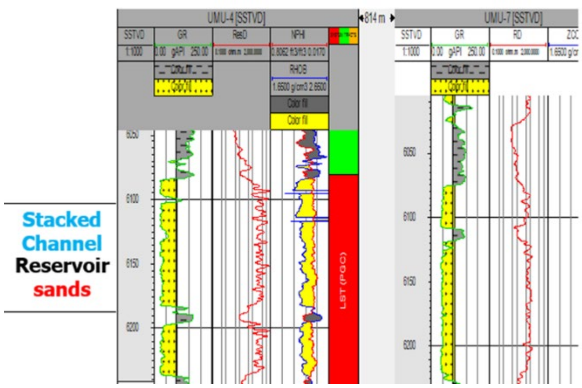

Fig. 11. Sands stacked in channel reservoirs in wells 1 and 3.

From the interpreted lithology (gamma ray) logs, the architectural style of the sand bodies showed strong aggradational stacking pattern, explained to be channel deposits (Figure 11). The observed boxy shape, with a frail fining upward sequence pattern, in the gamma-ray log reflects deposition in a fluvially-controlled channel. Nevertheless, shale intercalations in channel deposits results in reservoir disconnections and may impact fluid flow, thereby promoting vertical connectivity, as opposed to lateral connectivity.

5. Summary

The study has attempted the use of integrated interpretation of 3D seismic and well log data to re-appraise the identified hydrocarbon reservoir intervals mapped in the study area. Petrophysical evaluation results revealed that the average estimated porosity for each of the reservoirs decreased with increasing depth due to increasing sediment compaction. Hence, the wells' porosity ratings range from shallow areas with exceptional values to deeper areas that have acceptable porosity values.

The seismic horizons mapped in the field coincided with the tops of the reservoirs delineated from well log correlation, and were used to show the stratigraphic continuity of the sand bodies in both dip and strike directions. The interpreted faults were used to establish the structural framework and trapping mechanisms in the study area. Two of the faults (F2 and F4) were responsible for the formation of fault-dependent traps in the field. The estimated hydrocarbon reserves revealed that the field still holds considerable potentials for future exploration drilling.

6. Conclusion and recommendation

The identified prospects in the appraised reservoirs presents new prospect opportunities in the field. It is therefore necessary to launch drilling campaigns to test the potentials of these resource plays for marginal field revitalization.

References

[1] Okwudiri AA, Maduewesi CO, Ibemesi PO, and Okwara IC. Reservoir quality studies and prospect identification of a field in the Coastal Swamp Depobelt, Niger Delta. Pet Coal, 2017; 59(4): 505-515.

[2] Adewoye O, Amigun JO, Okwoli E, and Gwazan CA. Petrophysical and Structural Analysis of Maiti Field, Niger Delta, Using Well Logs and 3-D Seismic Data. Pet Coal, 2013; 55 (4) 302-310.

[3] Abbasi J, and Tabatabaei H. Investigating of Petrophysical and Lithological Parameters of Asmari Formation in Bibi-Hakimeh Oil Field, SW of Iran. Pet Coal, 2019; 61(4) 855-859.

[4] Short KC, Stauble AJ. Outline of geology of Niger Delta: American Association of Petroleum Geologists Bulletin. 1967; 51: 761-779

[5] Ekweozor CM, Okoye NV. Petroleum Source-bed evaluation of Tertiary Niger Delta: American Association of petroleum Geologists Bulletin, 1980; 64: 1251-1259

[6] Stacher P. Present understanding of the Niger Delta hydrocarbon habitat in Oti, M.N; and Postma, G; eds; Geology of Deltas: Rotterdam A.A. Balkema 1995, 257-267

[7] Evamy BD, Haremboure J, Kamerling P, Knaap WA, Molloy FA, Rowland, PH. Hydrocarbon habitat of Tertiary Niger Delta: American Association of Petroleum Geologists Bulletin 1978; 62: 1-39

[8] Orife IM, Avbovbo AA. Stratigraphic and Unconformity Traps in the Niger Delta in Halbouty M.T (ed).Deliberate search for subtle traps :American Association of Petroleum Geologists Memoir 1982; 32: 25-265

[9] Ladipo KO. Sequence stratigraphic analysis: An example of applications to prospect appraisal in the Northern (western) Niger Delta, Nigeria: Nigerian Association of Petroleum Explorationists Bulletin, 1992; 7: 153-158

[10] Opara GE. A review of the Tertiary Unam "B" Field in OML-67, Niger Delta: Journal of Mining and Geology, 1981; 18 (1): 86-95

[11] Asquith GB, Gibson CR. Basic well log analysis for geologist: American Association of Petroleum Geologist, 1982, Volume 3; DOI: https://doi.org/10.1306/Mth3425.

[12] Archie GE. The electrical resistivity log as an aid in determining some reservoir Characteristics: A Journal of Petroleum Technology, 1942; 146: 54-62.

[13] Ali ON, Jibriel A, and Essa MT. Estimation of Original Oil in Place for Belhadan Oil Field by Using Volumetric Method, Material Balance Equation Method, and Reservoir Simulation Method. The First Conference For Engineering Sciences and Technology 2018, https://doi.org/10.21467/proceedings.2.35.

To whom correspondence should be addressed: I. J Ofoh, Department of Geology, Federal University of Technology, P.M.B 1526, Owerri, Imo State, Nigeria; e-mail: ifeyinwaofoh@gmail.com